Methanogenesis by CO_2 reduction dominates lake sediments with different organic matter compositions

Guangyi Su[1*], Julie Tolu[2], Clemens Glombitza[3], Jakob Zopfi[4], Moritz F. Lehmann[4], Mark A. Lever[3], Carsten J. Schubert[1, 3]

[1] Swiss Federal Institute of Aquatic Science and Technology (EAWAG), Department of Surface Waters – Research and Management, 6047 Kastanienbaum, Switzerland

[2] Swiss Federal Institute of Aquatic Science and Technology (EAWAG), Department of Water resources and Drinking water, 8600 Duebendorf, Switzerland

[3] Institute of Biogeochemistry and Pollutant Dynamics, ETH Zurich, 8092 Zurich, Switzerland

[4] Department of Environmental Sciences, University of Basel, 4056 Basel, Switzerland

[*]corresponding author: Guangyi Su, guangyi.su@unibas.ch

Abstract

Microbial methane production is a respiration reaction involved in the terminal step of anaerobic degradation of organic matter. Due to the dependency of methanogenic substrate production on fermentation reactions that produce different end productions, different sources and compositions of organic carbon (OC) may impact the methanogenic potential in lake sediments. Here, we investigate the sources and compositions of OC in sediments of Lake Geneva and how both are potentially linked to methane production. Differences in dominant long-chain fatty acid abundances and carbon isotopic compositions suggest the predominance of diagenetically altered phytoplankton-derived OC at a profundal site and temporally highly variable sources of both aquatic and terrestrial OC in a deltaic location. Despite these differences, radiotracer-based methanogenesis rate measurements and stable isotopic signatures of methane indicate significant methane production that is dominated by CO_2 reduction (>95% of total methanogenesis) in both locations. Matching this interpretation, members of well-known CO_2-reducing *Methanoregula* sp. dominate both sites. No clear effect of OC source on methane production rates was evident. Our data demonstrate that OC of diverse sources and diagenetic states support microbial methane production, but do not indicate a clear impact of the OC source on the dominant methanogenic pathway or the community structure of methanogenic microorganisms in lacustrine sediments.

1. Introduction

Lakes represent an important source of methane (CH_4) to the atmosphere (Bastviken et al., 2011), which is a potent greenhouse gas with a global warming potential more than 27 times that of carbon dioxide on a 100-year basis (GWP-100) (Masson-Delmotte et al., 2021). Although recent evidence suggests that various living organisms can produce methane under oxic conditions (Ernst et al., 2022), most CH_4 in lakes is still produced primarily during the anaerobic decomposition of organic carbon (OC) in sediments, from where it escapes by ebullition or diffusion into the bottom waters. Methane formation is the final step in the degradation of organic matter, and is catalyzed by anaerobic methanogenic archaea, capable of using several substrates including H_2/CO_2, acetate, and methylated compounds (Lyu et al., 2018). It is still poorly understood how methane production in lake sediments is regulated, and to what extent the methanogenic potential is related to OC quality. In this regard, microbial organic matter degradation reactions (e.g., hydrolysis, fermentation, and anaerobic oxidation) play a critical role by sequentially breaking down organic macromolecules, such as proteins, carbohydrates, and lipids, to acetate and H_2/CO_2, which are then used as substrates by methanogenic archaea (Demirel and Scherer, 2008).

Freshwater lakes cover only a small portion of the Earth's surface (< 3%) (Downing et al., 2006), compared to oceans (71%), yet, the annually accumulated OC in lakes represents nearly half of what is stored in the oceans (Mendonça et al., 2017). In many lakes, most of organic matter in sediments is derived from autochthonous aquatic organisms like phytoplankton and aquatic macrophytes (Dean and Gorham, 1998). On the other hand, allochthonous organic carbon such as detritus of terrestrial vegetation can account for a significant fraction of the lacustrine sedimentary organic matter (Larsen et al., 2011), for example within river deltas (Randlett et al., 2015). In small or oligotrophic lakes and/or high-latitude/altitude lakes, OC sedimentation may in fact be dominated by land-derived organic matter, and it has previously been observed that high carbon burial efficiency in sediments is linked to a high proportion of allochthonous OC (Sobek et al., 2009). In general, OC from aquatic biomass such as

Deleted: A large fraction of

Deleted: produced in lakes

Deleted:

73 phytoplankton mainly comprises relatively labile compounds (Parsons et al., 1961). In

74 contrast, allochthonous OC (e.g., terrestrial plants) contains more complex structural

75 and biochemically recalcitrant compounds, such as cellulose and lignin (Opsahl and

76 Benner, 1995), which are more effectively preserved over time (Han et al., 2020, 2022).

77 The different biochemical compositions and characteristics of OC in lake sediments,

78 and the associated differential susceptibility to hydrolytic attack and microbial

79 breakdown into smaller carbon compounds (Lehmann et al., 2002, 2020), might

80 substantially affect CH_4 production and emission, as has been suggested in previous

81 studies (Grasset et al., 2018; West et al., 2012). However, laboratory experiments

82 performed at short-time scales (i.e., within weeks or months), involving the spiking of

83 sediments with fresh algal and/or plant organic materials, do not accurately reflect

84 effects of enhanced OC contribution to natural sediments on CH_4 production. This is

85 because the compositions and lability of original organic materials may vary greatly

86 after sedimentation due to oxidative destruction and microbial alteration during sinking

87 in the water column (Kawamura et al., 1987). Moreover, allochthonous OC found in

88 lake sediments is often the less-reactive (i.e. less bio-degradable) remnant of land-

89 derived debris, where the more reactive fractions have already been removed on land

90 or during fluvial transport (Raymond and Bauer, 2001). Lastly, while it is known that

91 organic matter bioavailability decreases over time, as labile components are selectively

92 remineralized (Grasset et al., 2018), the effects of organic matter quality and OC

93 degradation state, and their interactions, on CH_4 production remain uncertain.

94   Lipid biomarkers and their stable carbon isotopic composition can be used to infer

95 sources and diagenetic state of lacustrine organic matter (Dai et al., 2005; Meyers and

96 Ishiwatari, 1993). Different chain lengths of fatty acids and n-alkanes can be used for

97 the distinction between aquatic phytoplankton and terrestrial plants (Cranwell, 1976;

98 Eglinton and Hamilton, 1967). In addition, primary producers growing in different

99 habitats (e.g., terrestrial plants and freshwater phytoplankton) have distinct isotopic

100 compositions, due to the differences in C sources and biochemical pathways, through

101 which inorganic carbon is assimilated and incorporated into biomass (Cloern et al.,

102 2002). For example, terrestrial C3 plants incorporate carbon dioxide from the

103 atmosphere using the C3 Calvin-Benson pathway and consequently have an average

104 bulk isotopic value of ca -28‰, while isotopic values of various aquatic plants are often

105 significantly less negative (e.g., an average of -20‰ for benthic diatoms) (Cloern et al.,

106 2002; O'Leary, 1981). Moreover, stable carbon isotope measurements can be used to

trace the carbon flow from organic matter degradation to CH_4 in lake sediments. The isotopic signatures of methane and methane precursors (e.g., dissolved inorganic carbon, bulk organic carbon) can be used to assess the relative contribution of the major pathways (i.e., CO_2 reduction and acetoclastic methanogenesis) to total CH_4 production (Conrad, 2005; Whiticar, 1999). To date it remains unclear, which organic compounds represent the main precursors of molecules that are ultimately converted to methane in older sediments, in which more labile OC fractions, such as OC from microalgal cells, have largely been remineralized already. Previous research in Lake Geneva revealed higher benthic CH_4 fluxes, but lower total mineralization rates of organic matter in deltaic sediments, compared to profundal sites with reduced riverine impact (Randlett et al., 2015). The observed differences imply that despite less efficient total remineralization that leads to elevated OC burial rates in deltaic sediments, high CH_4 production is sustained due to the high input of allochthonous OC (Sollberger et al., 2014).

Here we investigated relationships between methanogenesis rates and pathways, and the sources and degradation state of sedimentary organic matter in profundal and deltaic sediments of Lake Geneva. We combined methanogenic rate measurements by radiotracer incubations with ^{14}C-labeled bicarbonate and acetate with compositional (lipids, pyrolysis-GC/MS) and stable carbon isotopic analyses of organic carbon and $CH4$, and sedimentation rate measurements (based on Pb-210, Cs-137). Additional quantitative analyses of a methanogenic marker gene (*mcr*A) and analyses of methanogenic community structure (16S rRNA gene sequences) provided insights into the abundances and identities of in situ methanogenic populations. Based on this multi-disciplinary data set, we identified potential relationships between sediment OC sources and degradation status, rates, pathways, and the organisms involved in the microbial production of methane.

2. Material and methods

2.1. Study sites

Lake Geneva is the largest western European lake. The Rhone River, the main tributary to the lake in the northeastern part, has a catchment area of 5220 km^2 and accounts for about 68% of the total water discharge and large amounts of suspended sediment and fine-particle loading to the lake (Burrus et al., 1989). The Rhone River

4

inflow brings in large amounts of terrestrial OC, which is mostly deposited near the river mouth as an important contribution to deltaic sediments. On the other hand, sedimentation in the deeper part of the lake is usually dominated by phytoplankton-derived OC (Gallina et al., 2017).

2.2. Sample collection and processing

Sediment cores were collected using a larger gravity corer (14 cm inner diameter) at a profundal site (46°25′54″N, 6°47′33″E, water depth: 240 m) and a smaller gravity corer (6.5 cm inner diameter) at a deltaic site (46°24′58″N, 6°51′34″E, water depth: 128 m) in August and December 2019, respectively. Profundal samples for different analyses were obtained from a single sediment core at 2-cm vertical resolution. Samples for the analysis of dissolved methane concentrations were collected on site with cut-off syringes through pre-drilled holes in the core liner covered with adhesive tape. Sediment samples of 2 cm^3 were fixed with 5 mL 10% NaOH in 120 mL serum bottles, which were capped immediately with thick butyl rubber stoppers and an aluminum crimp cap. Additionally, two replicate samples were taken from the same depth for methanogenesis rate measurements (described below). Sediment porewater was extracted with Rhizon samplers (Rhizosphere Research Products, Wageningen, Netherlands) connected to 20-mL syringes through predrilled small holes, with 2 cm distance between them. Porewater samples for DIC concentration measurements and stable carbon isotope analyses were stored in 4-mL glass vials without headspace at 4 °C. Separate porewater sample aliquots for the quantification of acetate and other volatile fatty acids were stored in combusted (450 °C for 5 h) glass vials at -20 °C until further analysis. The sediment core was then extruded in the lab and sectioned into 2 cm segments. Samples were taken from each segment and stored frozen (-20 °C) until further analysis for bulk parameters and lipid biomarkers. Using the gravity corer equipped with the smaller core liner, four sediment cores were obtained from the deltaic site. One core was used for methane concentration measurements, a second one for rate measurements (both at 2-cm resolution, sample collection as described above). The third core was used for porewater extraction in the lab using Rhizon samplers, and the last one was split open for the determination of porosity, analysis of bulk parameters and lipid biomarkers. An additional small-diameter sediment core was taken at the profundal site during the second sampling campaign for porosity analysis.

2.3. Rate measurements of methanogenesis using radiolabeled substrates

Methanogenesis rates (MGR) were determined using a radioisotope-based approach. We determined the modes of methane production and activity rates in incubation experiments with radio-labeled acetate and bicarbonate. At each depth, samples (2.5 cm^3) were collected through pre-drilled holes using 3 mL cut-off plastic syringes, which were closed with rubber stoppers and stored at 4 °C. Upon arrival of the samples in the laboratory, ten microliters of anoxic ^{14}C-labeled bicarbonate (~16 kBq, Perkin-Elmer) or 2-^{14}C-labeled (i.e., ^{14}C label in the methyl group) acetate solution (~18 kBq, Perkin-Elmer) were injected for the MGR measurements to determine CO$_2$ reduction (MGR$_{DIC}$) and acetoclastic (MGR$_{Ac}$) methanogenesis rates, respectively. Immediately after the tracer injection through the stoppers, all samples including killed controls (i.e., samples that were transferred to 10 mL 5% NaOH solution immediately after tracer injection) were incubated under an N$_2$ atmosphere at in situ temperature (4 °C) in the dark for 48 h.

To stop microbial activity in the incubations with ^{14}C-labeled substrates, samples were transferred into 120-mL serum bottles containing 10 mL aqueous NaOH (5% wt:wt), immediately crimp-sealed with butyl rubber stoppers and vigorously shaken. The ^{14}C activity in the different carbon pools was determined as previously described (Su et al., 2019). In brief, the headspace of a fixed sample is purged with air (30 mL min^{-1} for 30 min) through a heated (850 °C) quartz tube filled with copper oxide, where the ^{14}CH$_4$ (product of methanogenesis during incubation) is combusted to ^{14}CO$_2$. The ^{14}CO$_2$ is then captured in two sequential traps of scintillation vials (20 mL) containing 8 mL of 1:7 phenylethylamine and methoxyethanol. The cumulative radioactivity of both traps is then determined by liquid scintillation counting (2200CA Tri-Carb Liquid Scintillation Analyzer) after adding 8 mL of a scintillation cocktail (Ultima Gold, PerkinElmer) to each vial, and thorough mixing using a vortex-mixer. For incubations with bicarbonate, the residual ^{14}C-bicarbonate was measured as ^{14}CO$_2$, released from the alkaline liquid phase after adding 2.5 mL of 32% HCl. The remaining radioactivity (possibly explained by inorganic carbon assimilation into biomass) was determined in a 1-mL aliquot of the acidified mixture (amended with 4 mL Ultima Gold) by liquid scintillation counting. Incubation bottles with ^{14}C-acetate were also acidified with 2.5 mL of 32% HCl after extraction of ^{14}CH$_4$, and ^{14}CO$_2$ from microbial acetate oxidation was subsequently purged and trapped as described above. To determine the residual ^{14}C-acetate in the incubation vial, 1 mL of the acidified mixture was mixed with 4 mL

Deleted: carboxyl

Formatted: Superscript

Deleted: hydrogenotrophic

211 Ultima Gold for scintillation counting (Beulig et al., 2018). The control samples were
212 processed in the same way as the incubated samples after the termination of incubation.
213 The methanogenesis rates with DIC (nmol cm^{-3} d^{-1}) and acetate (nmol cm^{-3} d^{-1}) as
214 substrates were calculated using Eq. 1 and Eq. 2, respectively, modified from a previous
215 study (Beulig et al., 2018).

216 $$MGR_{DIC} = 1.08 \times \varphi \times [DIC] \times \frac{A_{CH_4}}{A_{CH_4} + A_{DIC} + A_R} \times t^{-1} \qquad (1)$$

217 $$MGR_{Ac} = 1.08 \times \varphi \times [Ac] \times \frac{A_{CH_4}}{A_{CH_4} + A_{DIC} + A_{Ac}} \times t^{-1} \qquad (2)$$

218 $[DIC]$ and $[Ac]$ are concentrations of DIC and acetate in the sediment porewater,
219 respectively. A_{CH_4} and A_{DIC} represent the activities of produced CH_4 and DIC (i.e.,
220 residual DIC in bicarbonate-amended incubations, product DIC in acetate-amended
221 incubations) at the end of the incubation (in CPM). A_R and A_{Ac} represent the remaining
222 radioactivity of DIC-incubated samples (i.e., biomass and metabolic intermediates) and
223 the residual ^{14}C-acetate radioactivity (possibly also including a small fraction of ^{14}C in
224 metabolic intermediates and incorporated into biomass), respectively. φ is the porosity
225 of the sediment samples. The factor 1.08 accounts for the isotopic fractionation of ^{14}C
226 (Hansen et al., 2001). t represents the incubation time in days. Measured $^{14}CH_4$
227 activities in all incubation samples were blank-corrected by subtracting the $^{14}CH_4$
228 activity measured in the killed control (typically close to background radioactivity)
229 incubated with the same amounts of ^{14}C-labeled substrates. The activities in the $^{14}CH_4$
230 pool were considered zero if the blank-corrected value was negative.

231

232 **2.4. Pore water methane and nutrient analyses**
233   Methane concentrations were measured in the headspace of NaOH-preserved
234 samples using a gas chromatograph (GC, Agilent 6890N) with a flame ionization
235 detector, and helium as a carrier gas. CH_4 concentrations in the wet sediments were
236 then calculated based on the headspace-to-sample volume ratio. The C isotopic
237 composition ($^{13}C/^{12}C$) of methane was determined in the same samples using a pre-
238 concentration unit (TraceGas, Micromass, UK) connected to an isotope ratio mass
239 spectrometer (IRMS; GV Instruments, Isoprime). Stable C-isotope values are reported
240 in the conventional δ notation (in ‰) relative to the Vienna Pee Dee Belemnite standard
241 (V-PDB), with a reproducibility of 0.5‰ based on replicate measurements of methane
242 standards. A carbon analyzer (TOC-L, Shimadzu, Kyoto, Japan) was used to quantify

dissolved inorganic carbon (DIC) concentrations in sediment porewaters. Samples were manually injected into the DIC reaction vessel and measured with a non-dispersive infrared detector (NDIR) after acidification and volatilization to CO_2. To determine the carbon isotopic composition of DIC, a porewater aliquot of 1-2 mL was introduced into a He-purged exetainer (Labco Ltd) and acidified with ~200 µL 85% H_3PO_4. After 2 h equilibration at 37 °C, the CO_2 released from the aqueous phase was subsequently analyzed using a preparation system (MultiFlow, Isoprime) coupled to an IRMS (Micromass, Isoprime). The standard deviation for replicate measurements of samples and standards was < 0.2‰. The apparent carbon isotope fractionation factor (α_c) during methanogenesis was estimated using $\delta^{13}C$ values of CH_4 and DIC (Eq. 3).

$$\alpha_c = \frac{1000 + \delta^{13}C-DIC}{1000 + \delta^{13}C-CH_4} \qquad (3)$$

Values of α_c greater than 1.065 were interpreted to indicate a predominance of CO_2 reduction over acetoclastic methanogenesis (Conrad, 2005). Porewater samples for acetate and other volatile fatty acids were analyzed with a two-dimensional ion chromatography (2D IC), as described previously (Glombitza et al., 2014), with modifications reported in (Schaedler et al., 2018). Samples were filtered through pre-washed (10 mL Ultrapure Type I water) disposable syringe filters (Acrodisc® IC grade, 0.2 µm pore size, 13 mm diameter). The first 0.5 mL sample after filtration was discarded before collecting the samples for 2D IC analysis. We used a dual Dionex ICS6000 instrument (Thermo Scientific) equipped with a Dionex AS24 column (2 mm diameter) for the first dimension, and a Dionex AS11HC column (2 mm diameter) for the second dimension. Quantification was done from the conductivity detector signal with a series of 5 external standards between 0.5 and 100 µM.

2.5. Bulk sediment analyses

The total organic carbon (TOC) contents of sediment samples were determined by the difference between total carbon and total inorganic carbon. Samples for total carbon were measured with an Elementar Vario Pyro Cube CN elemental analyser (Elementar, Germany), and samples for total inorganic carbon were analysed by coulometry using a UIC CM5015 coulometer (Joliet, IL, USA). Sediment cores were dated by gamma spectrometry using ^{137}Cs on freeze-dried and ground sediment for the determination of sedimentation rates, as described previously (Randlett et al., 2015). The $\delta^{13}C$-TOC was determined on decalcified samples (Schubert and Nielsen, 2000). Briefly, freeze-dried

277 and homogenized samples were treated with 5 mL 10% HCl in 15 mL Falcon tubes
278 overnight. After centrifugation, the supernatant was discarded, and the solid phase was
279 washed/centrifuged three times with 5 mL MilliQ water. Samples were dried at 50 °C
280 for 48 h prior to analysis. The δ^{13}C-TOC was then assessed by elemental analysis-
281 isotope ratio mass spectrometry (EA, Pyro Cube, Elementar and IRMS, Isoprime, UK).
282 The reproducibility based on replicate measurements of standards and samples was
283 better than 0.2‰.

285 **2.6. Pyrolysis gas chromatography-mass spectrometry**
286 The sedimentary organic matter composition was characterized at the molecular
287 level using a pyrolyzer equipped with an autosampler (EGA/PY-3030D and AS-1020E,
288 FrontierLabs, Japan) connected to a gas chromatograph (Trace 1310, Thermo
289 Scientific) and a mass spectrometer (ISQ 7000, Thermo Scientific), following the
290 optimized method (Tolu et al., 2015). Depending on the sample, an aliquot of 2-3 mg
291 of dry sediment was pyrolyzed at 450°C. A data-processing pipeline, including
292 chromatogram smoothing, alignment background correction and multivariate curve
293 resolution by alternate regression was used to automatically detect and integrate the
294 peaks and extract their mass spectra under "R" computational environment (R Core
295 Team, 2014). To optimize the number of detected peaks, data processing was
296 performed independently for the sediments from the deltaic site (DS) and the profundal
297 site (PS). Individual peaks were identified using "NIST MS Search 2" software which
298 includes the library "NIST/EPA/NIH 2011", complemented by spectra from published
299 studies. The relative abundances of these identified pyrolytic organic compounds
300 (Table S2) were calculated for each sample by normalization to the sum of their peak
301 areas set at 100%.

303 **2.7. Lipid extraction, separation, and quantification**
304 At both sites, sediment samples from five depths (1, 5, 11, 19, and 29 cm) were
305 selected based on redox conditions (1 cm: oxic/suboxic; all others anoxic), organic
306 carbon content, and methanogenesis rates (the latter two variables had peak value in the
307 deeper layers), then lyophilized and homogenized for subsequent lipid extraction. Prior
308 to extraction, an internal standard mix (5α-androstane, 3-eicosanone, n-C19:0 fatty acid
309 and n-C19 alkanol) was added to each sample for the quantification of single
310 biomarkers. Lipids were extracted in 20 mL of 7:3 Dichloromethane/Methanol

Deleted: Based on methanogenesis rate and geochemical profiles,…

Deleted: selected

Deleted: both locations

9

315 (DCM/MeOH) in a Microwave Reaction System (SolvPro, Anton Paar, Graz, Austria),
316 as described previously (Ladd et al., 2018). Total lipid extracts (TLEs) were obtained
317 by successively rinsing the samples with DCM after centrifugation, and then
318 concentrated using a Multivapor P-6 (Büchi Labortechnik AG, Switzerland). TLEs
319 were further evaporated to dryness, and saponified in 3 mL methanolic KOH-solution
320 (~1 N) at 80 °C for 3 h. Neutral compounds were extracted by liquid-liquid extraction
321 using hexane, fatty acids (FAs) were then extracted from the remaining aqueous phase
322 with hexane after acidification (pH < 2). The fatty acid fraction was treated using 1 mL
323 of BF_3 in methanol (14% v/v, Sigma Aldrich) at 80 °C for 2 h, and converted to fatty
324 acid methyl esters (FAMEs). Neutral compounds were further separated into four
325 different fractions using 500 mg/6mL pre-packed Si gel columns (filling
326 quantity/volume, Biotage, Uppsala, Sweden). Briefly, the neutral fraction was
327 dissolved in 4 mL hexane and transferred onto the column, followed by 4 ml
328 hexane/DCM (2:1 v/v), then 4 mL DCM/MeOH (19:1 v/v) and finally 4 mL MeOH,
329 with the elution of hydrocarbon, ketone, alcohol and remaining polar compounds,
330 respectively. The alcohol fraction was acetylated in 25 μL acetic anhydride and 200 μL
331 pyridine at 70 °C for 30 min.

332   All fractions were quantified using a gas chromatograph equipped with a flame
333 ionization detector (GC-FID) (GC-2010 Plus, Shimadzu, Japan). Samples were injected
334 onto an InertCap 5MS/NP column (0.25 mm × 30 m × 0.25 μm, GL Sciences, Japan)
335 using an AOC-20i autosampler (Shimadzu) through a split/splitless injector operated in
336 splitless mode at 280 °C. The column was heated from 70 °C to 130 °C at 20 °C min^{-1},
337 then to 320 °C at 4 °C min^{-1}, and held at 320 °C for 20 min. FAMEs were identified by
338 comparing their retention times to those of laboratory standards (i.e., a fatty acid methyl
339 ester mix and bacterial acid methyl ester from Supelco, reference no. 47885-U and
340 47080-U, respectively), and were quantified by normalization to the internal n-C19:0
341 fatty acid standard. Identification of hydrocarbons was performed by comparing their
342 retention times to those of an external standard containing C14 to C40 n-alkanes
343 (Sigma-Aldrich). The alcohols were characterized using a gas chromatography-mass
344 spectrometer (GC-MS, QP2020, Shimadzu, Japan) under identical chromatographic
345 conditions. Acquired mass spectra were identified through comparison with published
346 data.

347

348 **2.8. Compound-specific stable carbon isotope analysis**

349   The stable carbon isotope composition of FAMEs, n-alkanes and alcohols was
350   determined by gas chromatography-isotope ratio mass spectrometry (GC-IRMS), using
351   a Delta V Advantage IRMS (Thermo Scientific) with a ConFlow IV (Thermo
352   Scientific). Samples were injected with a TriPlus RSH autosampler to a PTV inlet
353   operated in splitless mode at 280 °C on a GC-1310 gas chromatograph (Thermo
354   Scientific, Bremen, Germany). The GC was equipped with a 30 m DB-5MS fused silica
355   capillary column (0.25 mm i.d., 0.25 μm film thickness). The GC oven was heated from
356   80 °C to 215 °C at 15 °C min^{-1}, then to 320 °C at 5 °C min^{-1}, and held at 320 °C for 10
357   min. Column effluent was combusted at 1020 °C. Compound-specific δ^{13}C values were
358   reported relative to the V-PDB scale, and calibrated externally using known δ^{13}C values
359   of an alkane mixture (n-C$_{17, 19, 21, 23, 25, 28 \text{ and } 34}$, Arndt Schimmelmann, Indiana
360   University, USA), which were run at the beginning and the end of each sequence, as
361   well as after every 6th sample injection. The standard deviation for replicate
362   measurements for these standards averaged 0.4‰, with the average offset from their
363   known values of less than 0.5‰. The isotopic values of FAMEs and acetylated alcohols
364   were additionally corrected for the introduction of carbon atoms during the
365   derivatization step.
366

367   **2.9. DNA extraction, PCR amplification, Illumina sequencing and data analysis**
368   DNA was extracted from selected sediment samples of Lake Geneva, where both
369   high and low methanogenic activities were detected (DS: 11, 19, 21 and 27 cm; PS: 5,
370   11, 19, and 29 cm), using FastDNA SPIN Kit for Soils (MP Biomedicals) following the
371   manufacturer's instructions. A two-step PCR approach was applied to prepare the
372   library for Illumina sequencing at the Genomics Facility Basel, as described in detail
373   previously (Su et al., 2020, 2023). PCR was performed using universal primers 515F-
374   Y and 926R targeting the V4 and V5 regions of the 16S rRNA gene. These primers
375   cover the majority (~84.7%) of the 16S rRNA gene sequences of methanogenic archaea
376   and are well-suited for assessing community structures of methanogens in
377   environmental samples (Table S4). Data were then analyzed with Phyloseq (McMurdie
378   and Holmes, 2013) in the R environment (R Core Team, 2014). Raw sequence data
379   were deposited at NCBI Short Read Archive under the Bioproject ID PRJNA736863
380   with accession numbers from SAMN19667760 to SAMN19667767.
381

382   **2.10. Quantitative PCR (qPCR)**

Deleted: were

Deleted: as

11

385   The abundance of methanogens in Geneva sediments was determined by qPCR
386 with the primer set mcrIRD and 2 μL DNA as template (Lever and Teske, 2015). qPCR
387 reactions of all DNA samples were performed using the SensiFAST SYBR No-ROX
388 Kit (Bioline) on a Mic (Magnetic Induction Cycler) real time PCR machine (Bio
389 Molecular Systems, Inc). An initial denaturing step of 95 °C for 3 min was followed by
390 40 cycles of 5 s at 95 °C, 10 s at 56 °C, and 22 s at 72 °C. The specificity of the
391 amplification was assessed by examining the melting curves from 72 °C to 95 °C. The
392 calibration curve was generated using a serial of 10-fold dilutions of pGEM-T Easy
393 plasmid DNA (Promega, USA) carrying a single copy of the target gene (mcrIRD-
394 F/mcrIRD-R). The number of gene copies in plasmid DNA was calculated using the
395 equation reported previously (Ritalahti et al., 2006). We further compared the absolute
396 gene copy numbers of *mcrA* between the two sites using the Wilcoxon signed-rank test
397 ('wilcox.test'), implemented in the R package 'stats' (R Core Team, 2014).
398

3. Results

3.1. Sediment geochemistry at the two study sites

401   The two sites displayed different hydro- and geochemical characteristics (Fig. 1
402 and Table S1 and Fig. S1). Dating of the sediments revealed that the deltaic site had a
403 slightly higher sedimentation rate (0.58 cm yr^{-1}) than the profundal site (0.43 cm yr^{-1}).
404 At the deltaic site (DS), two distinct peaks in methane concentration (~7 mM) were
405 observed at 9 and 23 cm, respectively (Fig. 1A). At the profundal site (PS),
406 concentrations of CH$_4$ increased with depth and remained relatively constant at ~4 mM
407 below 15 cm (Fig. 1E). At both sites, the pore water concentrations of dissolved
408 inorganic carbon (DIC) increased with depth, and considerable amounts accumulated
409 in the sediment pore water. The depth-integrated DIC concentrations in the top 30 cm
410 were 1964 mmol m^{-2} at PS and 3490 mmol m^{-2} at DS, however, based on the
411 sedimentation over the past 50 years, the depth-integrated DIC concentrations were
412 1302 mmol m^{-2} at PS (21 cm) and 3490 mmol m^{-2} at DS (29 cm). Acetate, as a potential
413 methanogenic substrate, showed concentration maxima of 25.9 μM (DS) and 3.8 μM
414 (PS) close to the sediment surface. The methane δ^{13}C values decreased with depth in
415 both deltaic sediments (from -64.9‰ to -72.2‰, Fig. 1B) and profundal sediments
416 (from -72.7‰ to -74.6‰, Fig. 1F). Overall, the observed methane carbon isotope values
417 at both sites fall within a range that is typical for biogenic production (Whiticar, 1999).

420   Vertical profiles of δ^{13}C-DIC show similar pattern at the two sites, with the lowest
421   values of -5.5‰ at 5 cm at DS (Fig. 1B) and -5.2‰ at 3 cm at PS (Fig. 1F). At PS, TOC
422   concentrations increase slightly with depth, with the mean content almost doubled
423   compared to DS (Fig. 1C and G, Table S1). With respect to its stable carbon isotope
424   composition, δ^{13}C-TOC increased slightly with depth at PS, from -28‰ in surficial
425   sediments to -26‰ below 7 cm whereas δ^{13}C-TOC values remained relatively constant
426   at DS throughout the sampled sediment column (~ -26‰). The elemental C/N ratios in
427   the sediments of DS show a very high variability with depth, and range from 6.7 to
428   16.8, with a mean value of 10.7 (Fig. 1D and Table S1), while the values at PS are
429   lower and less variant along the sediment core (7.9 ± 0.3, Fig. 1 H).

430
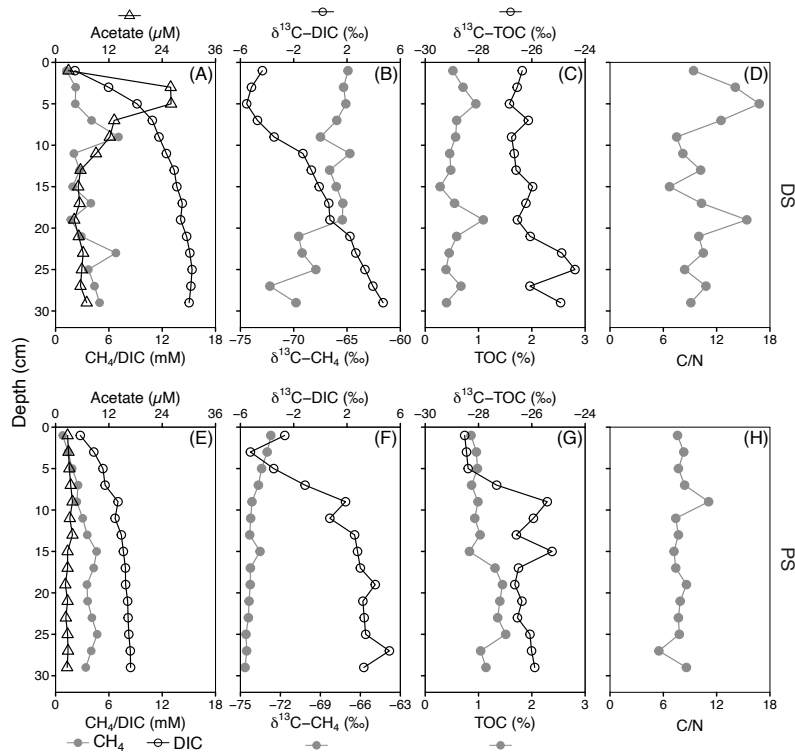
431
432   Figure 1. Sediment geochemistry as function of depth at a deltaic site (DS, A-D) and a
433   profundal site (PS, E-H) in Lake Geneva. (A, E) Profiles of dissolved methane,
434   dissolved inorganic carbon (DIC) and acetate concentrations. (B, F) Stable carbon
435   isotopic signatures (δ^{13}C) of CH$_4$ and DIC (in ‰ vs. V-PDB). (C, G) Concentrations of

436 total organic carbon (TOC, % of dry weight) and its carbon isotopic composition (in ‰
437 vs. V-PDB). (D, H) Molar ratios of total organic carbon to total nitrogen (C/N).
438

3.2. Composition of sedimentary organic matter

440   To investigate the molecular composition of sedimentary organic matter at the two
441 different sites, sediment samples were further analyzed using Py-GC/MS. We identified
442 a total of 65 individual organic compounds (Table S2), which can be classified into the
443 following compound groups: carbohydrates, N-compounds, n-alkenes, n-alkanes,
444 phenols, lignin oligomers, and (poly)aromatics. Both carbohydrates and N-compounds
445 were the most abundant organic compound groups among the pyrolysis products, with
446 no statistical difference between DS and PS (Fig. 2 A and B). At both sites, the
447 carbohydrates consisted mainly of compounds such as butenal, methylfuraldehyde and
448 furanone, and N-compounds were dominated by pyrrole, pyridine, methyl-pyrrole and
449 methyl-pyridine (Table S2), which are indicative of degraded products of carbohydrates
450 and proteins (Schellekens et al., 2009; Tolu et al., 2017). Most strikingly, sediments at
451 DS displayed significantly higher relative abundances of lignin ($p < 0.05$) and phenols
452 ($p < 0.01$) compared to profundal sediments (Fig. 3D and E). In addition, we observed
453 significantly higher relative abundances of n-alkenes at PS (Fig. 3C). This group
454 contains monounsaturated short-chain n-C_{15} to n-C_{18} (Table S2), which were the most
455 abundant organic compounds among the n-alkenes.
456

457
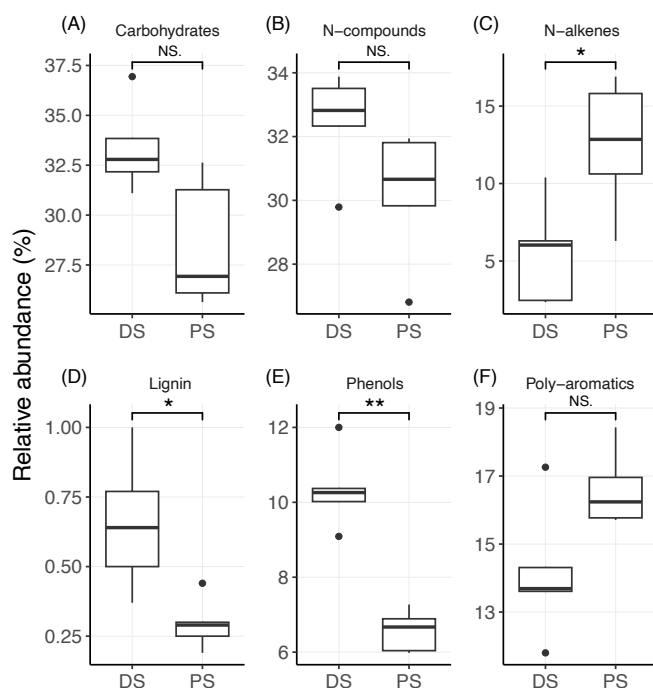
458　Figure 2. Relative abundances (in %) of different biochemical classes of organic

459　compounds in sediments at the deltaic (DS) and profundal site (PS) of Lake Geneva.

460　(A) Carbohydrates, (B) N-compounds, (C) N-alkenes, (D) Lignin, (E) Phenols and (F)

461　Poly-aromatics. Statistical differences of compound abundances between the two sites

462　were determined with the Wilcoxon signed-rank test. Significance levels are: ** $p<0.01$;

463　* $p<0.05$; NS. no significant differences between the two sites ($p>0.05$).

464

465　**3.3. Lipid concentration, distribution, and stable carbon isotopic signature**

466　　　Typical lipid biomarkers derived from aquatic phytoplankton (e.g., short-chain

467　fatty acids) and terrestrial plants (e.g., long-chain n-alkanes) were present in both

468　profundal and deltaic sediments, yet concentrations of some of these biomarkers were

469　strikingly different between the two sites, as well as between different depths within

470　the same site (Fig. 3 and Table S3). Among the fatty acids, n-$C_{16:0}$ was by far the most

471　abundant in all measured samples, with a slight increase in $\delta^{13}C$ values with depth at

472　both sites. At DS, the unsaturated fatty acids n-$C_{16:1\omega7}$ was the most abundant

473　monounsaturated fatty acids with the highest concentration observed at 11cm. At PS,

474　n-$C_{16:1}$ ($\omega7$ and $\omega5$) and n-$C_{18:1}$ ($\omega9$ and $\omega7$) decreased in concentration with depth and

15

were two to four times more abundant in the upper sediment layers (0-2 cm, 4-6 and 10-12 cm) than in the lower parts (18-20 and 28-30 cm). The short-chain fatty acids were generally depleted in ^{13}C, with stronger ^{13}C-depletions observed in surface sediments, particularly for the unsaturated fatty acids n-$C_{16:1\omega5}$ at PS.

In contrast to short-chain fatty acids, $C_{24:0}$ was most abundant among the long-chain fatty acids (i.e., $C_{24:0}$, $C_{26:0}$ and $C_{28:0}$), with relatively higher concentrations found in profundal sediments. Most strikingly, an apparent increase in the concentrations of these long-chain fatty acids was observed in the sediments of PS, with consistently high concentrations in the lower parts (10-30 cm). Meanwhile, the δ^{13}C values of these compounds decreased dramatically with depth. By comparison, concentrations of long-chain fatty acids at DS were variable at different sediment depths, but their δ^{13}C values remained relatively constant (e.g., $C_{28:0}$, Fig. 3B) and showed less variability with depth compared with PS (e.g., $C_{24:0}$ and $C_{26:0}$). Although the concentrations of long-chain n-alkanes at DS were twice as high as those at PS, their δ^{13}C values (particularly for C_{29}, C_{31} and C_{33}) were very similar at the two sites (Fig. 3B).

16
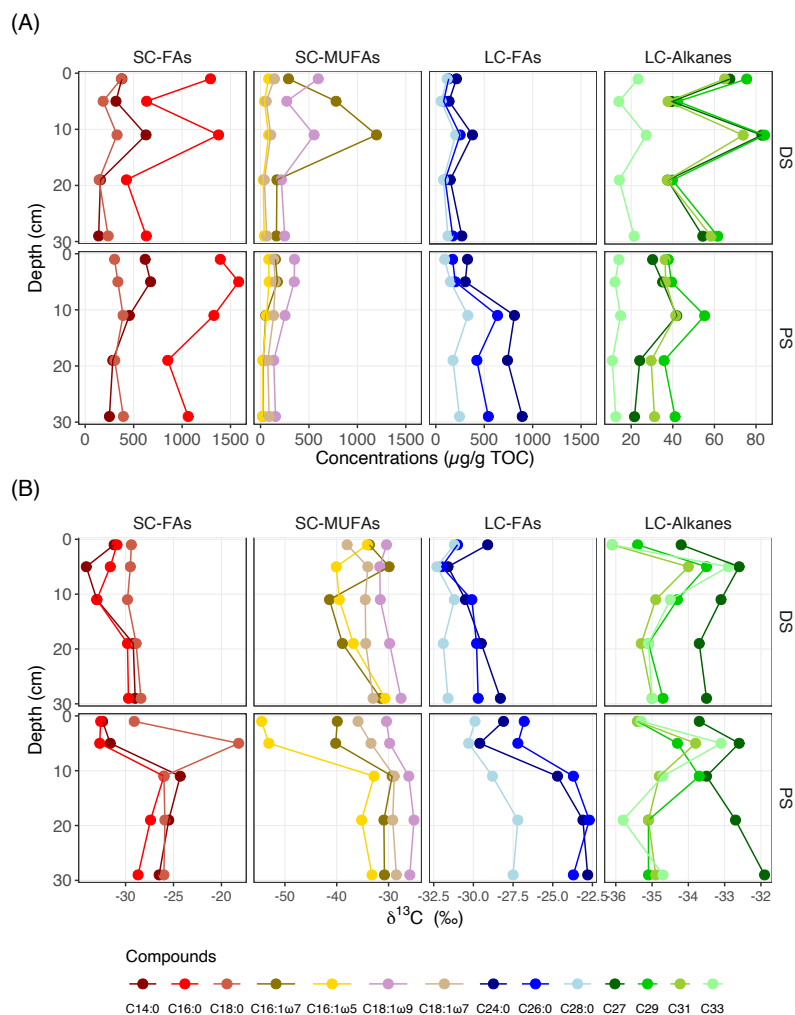
Figure 3. Vertical distribution of specific fatty acids and n-alkanes in deltaic (DS) and profundal (PS) sediments of Lake Geneva. (A) Concentrations (expressed as µg lipid g^{-1} TOC), and (B) compound-specific $\delta^{13}C$ values (in ‰ vs. V-PDB). SC-FAs, short-chain fatty acids ($C_{14:0}+C_{16:0}+C_{18:0}$); SC-MUFAs, short-chain monounsaturated fatty acids ($C_{16:1}$ and $C_{18:1}$); LC-FAs, long-chain fatty acids ($C_{24:0}+C_{26:0}+C_{28:0}$); LC-Alkanes, long-chain n-alkanes ($C_{27}+C_{29}+C_{31}+C_{33}$).

3.4. Relative importance of methanogenic pathways

499   Methane production through CO_2 reduction was observed at both sites and at all

500   depths. At the deltaic site, highest activity of CO$_2$ reduction methanogenesis was found

501   at the lower part of the sediment core (19-29 cm), while in the profundal sediment,

502   maximum rates of hydrogenotrophic methanogenesis were detected within the upper

503   sediments at depths between 7 and 17 cm (Fig. 4B and E, Table S1). In contrast, the

504   rates of methane production via acetate fermentation (i.e., acetoclastic methanogenesis)

505   were low, with maxima of 2.8 and 1.0 nmol cm^{-3} d^{-1} observed at 3 cm (PS) and 7 cm

506   (DS), respectively. The areal methanogenesis rates by CO_2 reduction within the top 30

507   cm, at both sites, were two orders of magnitude higher than acetoclastic methanogenesis

508   rates (Table S1). Acetate oxidation activity was very low at both PS and DS, with the

509   depth-integrated (0-30 cm) rates of 0.1 and 0.2 mmol m^{-2} d^{-1}, respectively (Table S1).

510   At both sites, the fractionation factor α_c, which is approximated based on the difference

511   between the measured δ^{13}C-DIC and δ^{13}C-CH$_4$ values, increased with depth (Fig. 4F),

512   ranging from 1.064-1.071 (DS) and 1.073-1.084 (PS).

513

514

Deleted: (i.e., hydrogenotrophic methanogenesis)

Deleted: hydrogenotrophic

Deleted: very
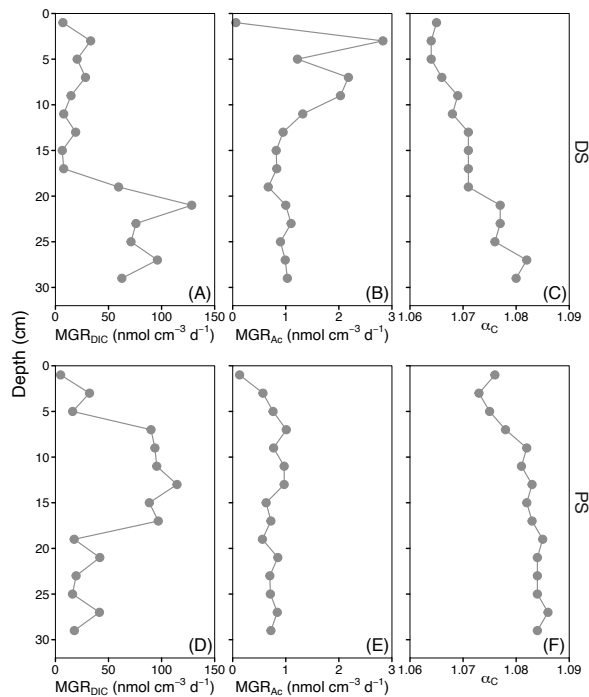
518   Figure 4. Depth profiles of (A, D) CO_2 reduction methanogenesis rates (MGR_{DIC}), (B,

519   E) acetoclastic methanogenesis rates (MGR_{Ac}), and (C, F) apparent fractionation factor

520   α_C in sediments of deltaic (DS) and profundal site (PS) in Lake Geneva.

521

3.5. Abundance and diversity of methanogenic archaea

523   On average, gene copy numbers of the methyl coenzyme M reductase gene (*mcrA*)

524   in the deltaic sediments of Lake Geneva were significantly higher than those in the

525   profundal sediments ($p < 0.05$; Fig. 5A). At both sites, *Methanoregula* and

526   *Methanothrix* dominated the methanogenic guild, followed by *Methanosarcina* and

527   *Methanobacterium* (Fig. 5B). Within the methanogenic community, the mean relative

528   abundances of *Methanothrix* and *Methanosarcina* were both higher at DS than those at

529   PS. By comparison, *Methanoregula* was the most abundant genus in the methanogenic

530   community at PS.

531
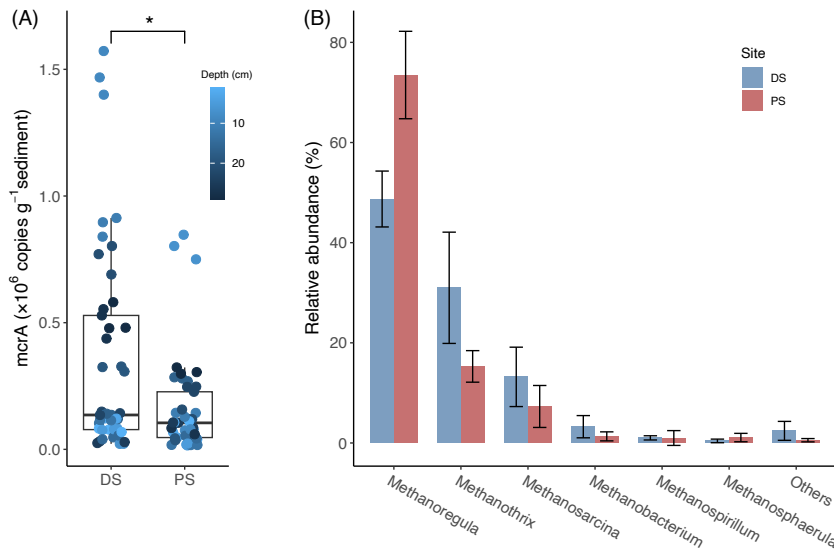
533   Figure 5. Abundance and diversity of methanogens at the deltaic (DS) and the profundal

534   site (PS) in Lake Geneva. (A) Absolute abundances of the *mcrA* gene encoding the α-

535   subunit of the methyl-coenzyme M reductase. Statistical difference between the two

536   sites was determined with the Wilcoxon signed-rank test and asterisk denotes

537   significance level (*: p<0.05). (B) Mean relative abundances of different methanogenic

538 groups (% of the total methanogens). Data are based on read abundances of 16S rRNA
539 gene sequences.

540

541 **3.6. Correlation analysis between geochemical parameters, methane production**
542 **rates, and microbial communities**

543   The alpha diversity measures indicate that the community structure of
544 microorganisms in the sediments at DS were more diverse than at PS (Fig. S2).
545 Principal coordinate analysis (PCoA) revealed significantly different microbial
546 community compositions at the two investigated sites, as indicated by the clear
547 separation of the data by the first principal coordinate, explaining 50.8% and 44.5% of
548 the observed variance for archaea and bacteria, respectively (Fig. S3). For both archaeal
549 and bacterial communities, PCoA plots show a very close aggregation of the deep
550 sediment samples at PS (17, 23 and 29 cm), indicating that their community structures
551 are highly similar. Conversely, there is quite some variance among the samples at the
552 more dynamic deltaic site DS, with its variable deposition history. The measured rates
553 of both CO_2 reduction and acetoclastic methanogenesis tend to be higher in sediment
554 samples harboring a more diverse microbial community (Fig. S4), but the relation is
555 weak and particularly for acetoclastic methanogenesis not significant. Pearson
556 correlation analysis between methane production rates and environmental parameters
557 show that methane production rates from both MGR_{DIC} and MGR_{Ac} was positively but
558 not significantly correlated with the concentration of short-chain n-alkanes (correlation
559 coefficients of 0.46 and 0.51 for MGR_{DIC} and MGR_{Ac}, respectively, Fig. S5). $\delta^{13}C\text{-}CH_4$
560 values showed a positive correlation with the abundance of carbohydrates, lignin, and
561 long-chain n-alkanes, and significant negative correlation with the abundance of long-
562 chain fatty acids and total organic carbon. C/N ratios were negatively correlated with
563 the concentrations of both short-chain and long-chain fatty acids (Fig. S5).

564

565 **4. Discussion**
566   Our results indicate a dominance of methane production by CO_2 reduction in both
567 profundal and deltaic sediments of Lake Geneva. This inference is supported by
568 radiotracer measurements, the observed apparent fractionation factors, and
569 methanogenic community analyses, which revealed members of CO_2-reducing
570 *Methanoregula* as the dominant group of methanogens. Thus, CO_2 reduction was

Deleted: s

observed as the primary MGR process both in sediments at PS, which predominantly contained diagenetically altered phytoplankton-derived OC, and sediments at DS characterized by variable sources of aquatic and terrestrial OC. We conclude, therefore, that the dominant pathway of methanogenesis does not primarily depend on the chemical composition of sedimentary organic matter. Other factors that affect production rates of different electron donors (e.g., H_2, acetate) could play a more important role, and will be discussed below.

4.1. Difference in organic carbon sources and diagenetic alteration

The deltaic sediments in this study displayed a strikingly large range of C/N ratios (6.7-16.8), whereas C/N ratios of profundal samples remained relatively constant throughout the sediment core (7.9 ± 0.3). Fresh organic matter from lacustrine phytoplankton, which is protein- rich (Parsons et al., 1961), typically has low C/N ratios of 6-9 (Meyers and Ishiwatari, 1993). In contrast, bulk sediment containing large portions of terrestrial vascular plants often displays much higher C/N ratios, sometimes at least three times greater, due to its high content of high-carbon structural components and refractory organics such as lignin (Hedges et al., 1986). A comparison of carbon isotope and bulk C/N values to data from previous studies (Lamb et al., 2006) confirmed the presence of both aquatic and terrestrial sources in the deltaic sediments, and the dominance of organic matter of autochthonous origin (e.g., algal biomass) at PS (Fig. 6). At DS, variable microbial community structures and significant changes in C/N ratios with depth reflect a highly variable depositional history, indicating differing origins of sedimentary organic matter. Specifically, peak C/N ratios of 16.8 at 5 cm and 15.4 at 19 cm were likely derived from terrestrial organic matter in these intercalated layers, while relatively lower ratios (~10) at other depths suggest a mixture of aquatic and terrestrial sources. Even lower values (~7) in some deltaic sediment layers may indicate predominantly autochthonous deposition of phytoplankton particles.
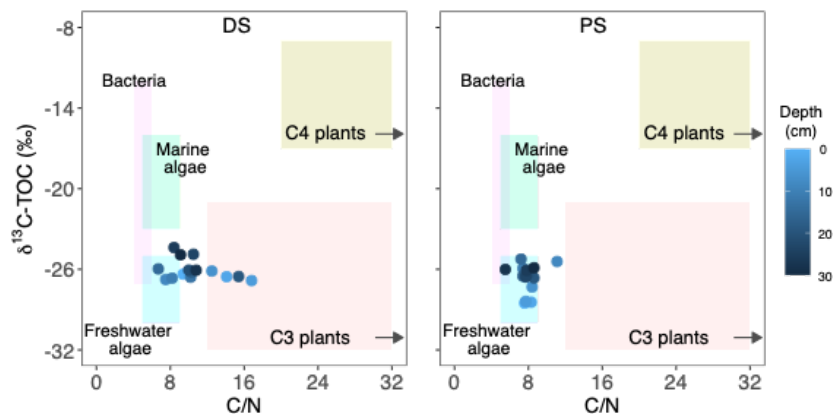
21

Figure 6. Comparison of $\delta^{13}C$ and bulk C/N values of Lake Geneva sediments from the deltaic (DS, left) and profundal site (PS, right) to elemental and isotopic indicators of bulk organic matter produced by bacteria, marine and freshwater algae, as well as terrestrial C3 and C4 plants (Lamb et al., 2006).

Indeed, at both sites, sediments contained OC from aquatic biomass, as verified by the short-chain fatty acids, indicative of freshwater algae (Cranwell, 1976), and/or in situ production by bacteria (Volkman et al., 1998). However, contrary to the findings from the combined carbon isotope and bulk C/N ratios, both lignin/phenols (Fig. 2) and long-chain n-alkanes (Fig. 3A) derived from terrestrial plants were detected in profundal sediments, although the concentrations of these compounds were lower at PS than at DS. Long-chain fatty acids (i.e., $C_{24:0}$ and $C_{26:0}$), which are typically assumed to originate from terrestrial plant waxes (Cranwell, 1974), make up a proportionally more important fraction of lipids in deeper sediment layers, particularly below 5 cm depth. However, the distinct carbon isotope compositions of these long-chain fatty acids between the two sites (Fig. 3B and Table S3, $\delta^{13}C$ on average ~7‰ lower at DS than at PS) suggest different OC sources.

Indeed, Chikaraishi et al. (2004) reported that long-chain fatty acids (i.e., $C_{24:0}$ and $C_{26:0}$) have $\delta^{13}C$ values of -36.3±2.6‰ for a variety of terrestrial vascular plants, whereas the $\delta^{13}C$ for aquatic plants is significantly less negative (-25.5±0.9‰). At PS, $\delta^{13}C$ values for $C_{24:0}$ and $C_{26:0}$ fatty acids (below 5 cm depth) were close to those indicative of freshwater aquatic plants (Chikaraishi et al., 2004). Previous studies have shown that both aquatic macrophytes and microalgae may represent potential sources

22

624   of long-chain fatty acids (Ficken et al., 2000; Volkman et al., 1998). However, it seems

625   somewhat contradictory to conclude that long-chain fatty acids were primarily derived

626   from aquatic vascular plants, simply because the observed C/N ratios at PS were too

627   low. Indeed, microalgae such as diatoms were estimated to contribute from 30-80% of

628   the $C_{24:0}$ to $C_{28:0}$ fatty acid pool in intertidal sandy sediment (Volkman et al., 1980).

629   Thus, the long-chain fatty acids observed in the profundal sediments may also have

630   been derived from microalgae (Volkman et al., 1998). This, in turn, could explain why

631   TOC was more depleted in ^{13}C in the surface sediments at PS, which does not

632   necessarily indicate the origins of terrestrial plants (Cloern et al., 2002).

633   The carbon isotopic composition of long-chain n-alkanes (i.e., C_{27-31}),

634   characteristic for land-derived organic matter (Chikaraishi et al., 2004), was almost

635   identical between PS and DS (Fig. 3B, ranging from -35‰ to -33‰), suggesting a

636   similar terrestrial source. At DS, if long-chain n-alkanes and long-chain fatty acids were

637   derived from the same terrestrial source, they should have similar C-isotopic values.

638   However, the slightly lower δ^{13}C values of long-chain fatty acids at DS (on average, -

639   30‰) imply a mixture of both aquatic and terrestrial sources, which is consistent with

640   the C/N ratios observed at this site.

641   Turning to other OM biomarkers, phytol concentrations were considerably higher

642   at PS (with no clear depth trend) compared to DS, whereas no clear difference in

643   cholesterol concentrations was observed between the sites (with depth-dependent

644   concentration decrease at both sites). For brassicasterol, there seems to be a clear depth-

645   related decrease at both sites, with slightly higher concentrations in surface sediments

646   (0-2 and 4-6 cm) at PS compared to DS. Phytol, a side chain of chlorophyll, can

647   originate from both phytoplankton and terrestrial plants (Shi et al., 2001). Due to its

648   rapid degradation under intense-light and oxic conditions in terrestrial environments,

649   terrestrially derived phytol (or chlorophyll) is generally of minor importance in aquatic

650   sediments (Meyers and Takeuchi, 1981), so it can be assumed that most of the

651   sedimentary phytol is derived from aquatic sources (Ladd et al., 2018). As for

652   cholestanol and brassicasterol (Table S3), the former can originate from both

653   zooplankton and phytoplankton (Bechtel and Schubert, 2009), while the latter is a lipid

654   biomarker mainly derived from phytoplankton in aquatic sediments (Volkman, 1986).

655   Hence, based on at least two of the biomarkers presented here, we have putative

656   evidence for a shift towards more autochthonous OM at the profundal site, as could be

657   expected.

658

4.2. Methanogenesis is mainly driven by CO_2 reduction

659

660   Our rate measurements using trace ^{14}C-labelled substrates clearly showed that CO_2

661   reduction played a dominant role in methane formation in both the PS and DS

662   sediments, compared to acetoclastic methanogenesis. As we did not measure rates of

663   methylotrophic methanogenesis, we are unable to determine the relative importance of

664   this pathway. However, since we neither detected common methylated compounds

665   such as methanol in the sediment porewater, nor methanogens that exclusively perform

666   methylotrophic methanogenesis at any of the studied sites, we argue that this pathway

667   is likely of a minor importance with regards to its the contribution to the overall

668   methane production at these sites. Indeed, H_2/CO_2 and acetate are usually the main

669   substrates in freshwater environments (Lyu et al., 2018), and to date, no direct evidence

670   for the occurrence of methylotrophic methanogenesis has been documented for lake

671   sediments. Methylotrophic methanogenesis has been shown to be an important pathway

672   mainly in specific marine systems, where methanogens can utilize methylated

673   compounds (e.g., methanol and trimethylamine) as non-competitive substrates for

674   methane production (Xiao et al., 2018; Xu et al., 2021; Zhuang et al., 2018).

675   The finding that CO_2 reduction pathway dominated methane production

676   throughout the sediment cores at both sites was further supported by the observed

677   apparent fractionation factor α_c (DS: 1.071 ± 0.001 and PS: 1.081 ± 0.001; Fig. 4C, F

678   and Table S1). Rates for CO_2 reduction in Lake Geneva were similar at the two studied

679   sites, but were much higher than those previously reported in other lakes at similar

680   depths (Kuivila et al., 1989). The observed low rates for acetoclastic methanogenesis

681   on the other hand were comparable to those in other lake sediments (Kuivila et al.,

682   1989; Schulz and Conrad, 1996). Methane production via acetate fermentation was

683   traditionally believed to play a more important role than via CO_2 reduction in lake

684   sediments (Whiticar, 1999; Whiticar et al., 1986). However, more recent evidence

685   seems to contradict this paradigm, demonstrating that CO_2 reduction methanogenesis

686   can indeed be a much more significant methane-producing biogeochemical pathway

687   than acetoclastic methanogenesis (Blair et al., 2018; Conrad et al., 2011; Meier et al.,

688   2024). While the dominance of CO_2 reduction methanogenesis in lake sediments has

689   been reported previously, our results reinforce this conclusion with consistent

690   geochemical and isotopic evidence across contrasting sedimentary regimes in Lake

691   Geneva.

Deleted: hydrogenotrophic

Deleted: The predominance of methane formation via CO_2 reduction over acetoclastic methanogenesis is an important finding, which, in Lake Geneva, appears to apply to sediments across different sedimentary depositional regimes.

Deleted: i.e.,

24

At both sites, *Methanoregula* was the most abundant methanogenic genus, particularly in deep sediments where the highest CO_2 reduction rates were observed. This genus, commonly found in freshwater lakes (Bartosiewicz et al., 2024; Berberich et al., 2020; Meier et al., 2024), is known to perform hydrogenotrophic methanogenesis (i.e., CO_2 reduction with hydrogen as the electron donor). *Methanothrix*, the second most abundant methanogen, primarily performs acetoclastic methanogenesis. At PS, *Methanoregula* dominated at all investigated depths, in accordance with high rates of autotrophic methanogenesis. While acetoclastic methanogenesis played only a minor role in total methane production, higher rates were observed for deltaic sediments, with lower apparent fractionation factor. This observation is consistent with higher concentrations of acetate and a higher relative abundance of acetate-consuming *Methanothrix*, suggesting that the pathway of acetoclastic methanogenesis was influenced by both the availability of acetate and the functional methanogenic population. While *Methanothrix* has long been considered to exclusively use acetate as substrate for methanogenesis (Jetten et al., 1992; Smith and Ingram-Smith, 2007), there is now evidence that some species can also perform CO_2 reduction via direct interspecies electron transfer (Rotaru et al., 2014; Zhou et al., 2023).

Although overall methane production rates were similar at both sites, the qPCR data in hand indicated that bulk methane production was not primarily controlled by (i.e., proportional to) the cell abundance of methanogens. Instead, it was likely regulated by other environmental factors, such as limited substrate supply (i.e., H_2 and acetate), stemming from rates of hydrolysis (Kristensen et al., 1995) and/or fermentation rates (Valentine et al., 1994) within the sediments. Since methanogens rely on syntrophic and other heterotrophic bacteria to generate these key substrates, the activity and composition of the broader microbial community may play a significant role in shaping methane production rates (Beulig et al., 2018; Liu and Whitman, 2008). In Lake Geneva sediments, rates of both CO_2 reduction and acetoclastic methanogenesis increased with microbial Shannon diversity. More diverse microbial communities tend to possess more diverse organic matter degradation capacities, resulting in higher production of acetate and H_2/CO_2, which in turn promotes overall methane production (Conrad, 2020). In addition, our microbial abundance and diversity data were insufficient to fully characterize the carbon metabolism of microorganisms involved in H_2 and acetate production, which could directly impact CO_2 reduction and acetoclastic methanogenesis and potentially explain the observed methane production

25

747 differences. The very low acetate oxidation rates at both sites suggest that differences
748 in methane generation via MGR_{DIC} versus MGR_{Ac} may be attributed to the relative
749 availability of methane precursors available (i.e., H_2/CO_2 versus acetate) (Capone and
750 Kiene, 1988). The acetate concentrations were below 26 µM at both sites, but well
751 within the range of what has been measured in profundal sediment of Lake Constance,
752 where acetoclastic methanogenesis was dominant (Schulz and Conrad, 1996). Hence,
753 the consistently low rates of acetoclastic methanogenesis throughout the sediment cores
754 at both sites likely resulted from low turnover rates of acetate during organic matter
755 degradation.
756
4.3. Effect of organic carbon characteristics on methanogenesis
758 Despite the differences in OC sources and quality between the two sites, the overall
759 methane production rates were comparable (Fig. 4B, E and Table S1). However, the
760 sedimentary zones of maximum methane production and the depth-dependent rates of
761 both metabolic modes of methanogenesis varied. This likely reflects differences in OC
762 quality and degradation pathways, which influence the balance between
763 remineralization to H_2/CO_2 versus acetate (Conrad, 2020), resulting in spatial
764 variability in sedimentary methane production.
765 Potential methane production rates have been shown to correlate positively with
766 the quantity of sediment organic matter (Berberich et al., 2020). However, at both the
767 DS and PS in Lake Geneva, the sediment layers of maximum rates of CO_2 reduction
768 did not coincide with higher TOC contents. Instead, combined rate and isotopic
769 measurements revealed that methanogenesis rates via CO_2 reduction corresponded to
770 less ^{13}C-depleted bulk organic carbon (Fig. 1 and 4). This suggests that the source and
771 microbial decomposition of organic matter, rather than its quantity, primarily
772 influenced the methanogenic activity via the CO_2-reduction pathway.
773 Methane production rates in lake sediments can be quite low across various
774 latitudes but can also increase significantly with the addition of fresh organic carbon
775 (Bartosiewicz et al., 2024; Schwarz et al., 2008; West et al., 2012). Indeed, high lipid
776 contents in phytoplankton biomass have been shown to enhance methane production in
777 both engineered systems and lake sediments (West et al., 2015; Zhao et al., 2014).
778 Additionally, existing evidence suggest that terrestrial OC can stimulate methane
779 ebullition in reservoirs (DelSontro et al., 2011; Sobek et al., 2012). It has also been
780 suggested that the availability of easily degradable organic matter controls both

26

Deleted: low (

Deleted:)

Deleted: are generally

Formatted: English (UK)

Formatted: English (UK)

Deleted: Our findings from rate measurement and organic carbon composition agree with earlier studies, indicating that both aquatic and terrestrial OC can significantly contribute to methane production .

788 methanogenic pathways and methanogenic archaeal communities (Liu et al., 2017).
789 However, the influence of organic matter source or composition on the relative
790 importance of methane production pathways and their corresponding rates remains
791 poorly constrained and has rarely been explored. At PS, within the zone of high
792 methanogenic activity via CO_2 reduction, TOC became less depleted in ^{13}C, a trend
793 also observed, though less pronounced, in the deltaic sediments. The $\delta^{13}C$ shift of TOC
794 within the most active zone at PS likely reflects either the selective loss of isotopically
795 light OM fractions, or changes in organic matter sources, as indicated by depth-related
796 variations in both short- and long-chain fatty acid concentrations.

797 Contrary to previous studies demonstrating that algal deposition stimulated the
798 activity of acetoclastic methanogens (Schulz and Conrad, 1995; Schwarz et al., 2008),
799 our results revealed higher acetate concentrations in tandem with higher acetoclastic
800 methanogenesis occurring in surface sediments of deltaic site, where high C/N ratios
801 indicated terrestrial inputs. This suggests that allochthonous OC may play a role in
802 acetate production and acetoclastic methanogenesis. However, the apparently much
803 lower overall acetoclastic rates compared CO_2 reduction were likely due to the active
804 acetate consumption via syntrophic oxidation (Conrad et al., 2020). At PS,
805 autochthonous organic matter was the dominant OC source to the sediments, and the
806 CH_4 produced likely resulted from the decomposition of buried algal detritus (Fig. 6).
807 This interpretation is also supported by the 2-fold higher brassicasterol, the 3-fold
808 higher phytol, and 3-4-fold higher long chain fatty acids concentrations (with elevated
809 $\delta^{13}C$ values) at PS compared to DS. These biomarkers, in combination with lower C/N
810 ratios, are indicative of algal material as the dominant organic contributor to early
811 diagenetic methane production.

812 While the dominant sedimentary organic matter source (i.e., the partitioning
813 between autochthonous versus allochthonous OM inputs to the sediments) varied
814 between the two studied sites, the similar overall methane production rates imply that
815 methanogenesis occurred ubiquitously in these lacustrine sediments, independent of the
816 OC sources, their apparent susceptibility to organic matter degradation, and/or their
817 overall diagenetic state. This finding aligns with a recent study across the river/deltaic-
818 pelagic continuum in a reservoir system in southwest Ohio (Berberich et al., 2020), and
819 holds important implications for understanding the lacustrine methane cycle. On the
820 one hand, eutrophication in lakes and other aquatic systems often increases the supply
821 of autochthonous organic carbon, thereby enhancing methanogenesis and leading to

829 increased methane emissions (Davidson et al., 2018). On the other hand, the potential
830 of terrestrial organic matter to contribute to lacustrine methane production can be
831 significantly impacted by anthropogenic activities, such as dam construction (Li et al.,
832 2023), or as a result of deforestation and soil erosion, which alter sediment inputs into
833 the lake (Bélanger et al., 2017). Our study demonstrates that diverse OC sources and
834 varying diagenetic states in both profundal and deltaic sediments support substantial
835 rates of methane formation through CO_2 reduction. However, identifying the exact
836 fractions of organic matter that were degraded and fueled methane production remains
837 challenging. While acetoclastic methanogenesis appears to be relevant to the break-
838 down and decomposition of terrestrial organic matter that favors acetate production and
839 accumulation in deltaic sediments, the sources of organic carbon driving the more
840 dominant CO_2-reducing methanogenesis in the studied sediments remains unclear. The
841 key environmental factors controlling the organic matter degradation in methanogenic
842 sediments remain unresolved and require further investigation. Understanding these
843 mechanisms is essential for predicting how changes in organic carbon inputs and
844 sediment dynamics may influence methane production and emissions from lacustrine
845 environments.
846

847 **5. Conclusions**

848 Our study demonstrates that both profundal and deltaic sediments of Lake Geneva
849 are significant sources of methane, despite clear differences in origins and compositions
850 of organic matter. The profundal site is dominated by aquatic OM, while the deltaic site
851 features a more variable mix of OM sources, including substantial terrestrial
852 contributions at certain depths. Methane production at both sites is driven by CO_2
853 reduction, which accounted for over 95% of total methane production and was most
854 probably mediated by *Methanoregula*. While phylogenetic data suggest a link between
855 methanogen communities and methanogenetic pathways, the broader microbial
856 community dynamics, particularly those involved in H_2 and acetate production, remain
857 insufficiently understood.

858 At the profundal site, methane production is mainly associated with the
859 decomposition of aquatic organic matter, as terrestrial OC is less abundant. At the
860 deltaic site, acetoclastic methanogenesis appears linked to the higher terrestrial organic
861 matter inputs. Nevertheless, the overall dominance of methanogenesis via CO_2

Deleted: Difference in the source and lability of organic carbon in the lacustrine organic matter pool may affect sediment methane production in distinct ways .

Deleted: overwhelmingly

866 reduction at both sites suggests that depositional regime, as well as OM source and
867 composition are not the primary determinants of the prevailing methane producing
868 pathway. Instead, other environmental factors such as substrate availability or
869 microbial community dynamics may influence methane production, although the
870 specific mechanisms remain uncertain. For example, the sample-specific molecular
871 composition of sedimentary organic matter could be important in determining which
872 substrate, H_2 and acetate, is the main substrates for methanogenesis. Future research
873 should focus on unraveling these interactions to better predict if, and how, changes in
874 OM inputs and sediment dynamics may impact methane emissions from lacustrine
875 environments.
876

Deleted: Instead, factors such as the metabolic interactions within microbial communities (e.g., with syntrophic partner organisms), particularly the balance of H_2 and acetate production, may play a larger role.

Data availability statement

Raw reads of the 16S rRNA sequencing data are available on NCBI GenBank with BioProject ID PRJNA736863, under accession number SRR14794332- SRR14794339.

Author contributions

CJS, GS and MAL conceived the research. CJS acquired funding for this study. GS performed field work, lab experiments and data analyses. JT assisted with Pyrolysis-GC data analysis. CG and MAL measured porewater volatile fatty acids and analyzed the data. JZ and MFL supported rate measurements and molecular analyses. GS wrote the original draft of the manuscript. All authors helped to revise and approved the submitted version.

Acknowledgements

This research was supported by Eawag internal funds. We thank Alois Zwyssig, Sandra Schmid and Cameron Callbeck for assistance with field sample collection. We also thank Serge Robert for laboratory assistance including lipid sample preparation and laboratory analyses and for his help in elemental analysis of samples. Patrick Kathriner is acknowledged for laboratory support. We are also grateful to Thomas Kuhn at the University of Basel for laboratory support with the radioisotope measurements.

Competing interests

At least one of the (co-)authors is a member of the editorial board of Biogeosciences.

References

Bartosiewicz, M., Przytulska, A., Birkholz, A., Zopfi, J., and Lehmann, M. F.: Controls and significance of priming effects in lake sediments, Glob Chang Biol, 30, 1–13, https://doi.org/10.1111/gcb.17076, 2024.

Bastviken, D., Tranvik, L. J., Downing, J. A., Crill, P. M., and Enrich-Prast, A.: Freshwater methane emissions offset the continental carbon sink, Science (1979), 331, 50–50, https://doi.org/10.1126/science.1196808, 2011.

Bechtel, A. and Schubert, C. J.: A biogeochemical study of sediments from the eutrophic Lake Lugano and the oligotrophic Lake Brienz, Switzerland, Org Geochem, 40, 1100–1114, https://doi.org/10.1016/j.orggeochem.2009.06.009, 2009.

Bélanger, É., Lucotte, M., Moingt, M., Paquet, S., Oestreicher, J., and Rozon, C.: Altered nature of terrestrial organic matter transferred to aquatic systems following deforestation in the Amazon, Applied Geochemistry, 87, 136–145, https://doi.org/10.1016/j.apgeochem.2017.10.016, 2017.

Berberich, M. E., Beaulieu, J. J., Hamilton, T. L., Waldo, S., and Buffam, I.: Spatial variability of sediment methane production and methanogen communities within a eutrophic reservoir: Importance of organic matter source and quantity, Limnol Oceanogr, 65, 1336–1358, https://doi.org/10.1002/lno.11392, 2020.

Beulig, F., Røy, H., Glombitza, C., and Jørgensen, B. B.: Control on rate and pathway of anaerobic organic carbon degradation in the seabed, Proc Natl Acad Sci USA, 115, 367–372, https://doi.org/10.1073/pnas.1715789115, 2018.

Blair, N. E., Leithold, E. L., Thanos Papanicolaou, A. N., Wilson, C. G., Keefer, L., Kirton, E., Vinson, D., Schnoebelen, D., Rhoads, B., Yu, M., and Lewis, Q.: The C-biogeochemistry of a Midwestern USA agricultural impoundment in context: Lake Decatur in the intensively managed landscape critical zone observatory, Biogeochemistry, 138, 171–195, https://doi.org/10.1007/s10533-018-0439-9, 2018.

Burrus, D., Thomas, R. L., Dominik, J., and Vernet, J.-P.: Recovery and concentration of suspended solids in the upper rhone river by continuous flow centrifugation, Hydrol Process, 3, 65–74, https://doi.org/10.1002/hyp.3360030107, 1989.

Capone, D. G. and Kiene, R. P.: Comparison of microbial dynamics in marine and freshwater sediments: Contrasts in anaerobic carbon catabolism, Limnol Oceanogr, 33, 725–749, https://doi.org/10.4319/lo.1988.33.4part2.0725, 1988.

Chikaraishi, Y., Naraoka, H., and Poulson, S. R.: Hydrogen and carbon isotopic fractionations of lipid biosynthesis among terrestrial (C3, C4 and CAM) and aquatic plants, Phytochemistry, 65, 1369–1381, https://doi.org/10.1016/j.phytochem.2004.03.036, 2004.

Cloern, J. E., Canuel, E. A., and Harris, D.: Stable carbon and nitrogen isotope composition of aquatic and terrestrial plants of the San Francisco Bay estuarine system, Limnol Oceanogr, 47, 713–729, https://doi.org/10.4319/lo.2002.47.3.0713, 2002.

Conrad, R.: Quantification of methanogenic pathways using stable carbon isotopic signatures: a review and a proposal, Org Geochem, 36, 739–752, https://doi.org/10.1016/j.orggeochem.2004.09.006, 2005.

Conrad, R.: Importance of hydrogenotrophic, aceticlastic and methylotrophic methanogenesis for methane production in terrestrial, aquatic and other anoxic

963   environments: A mini review, Pedosphere, 30, 25–39,
964   https://doi.org/10.1016/S1002-0160(18)60052-9, 2020.
965   Conrad, R., Noll, M., Claus, P., Klose, M., Bastos, W. R., and Enrich-Prast, A.: Stable
966   carbon isotope discrimination and microbiology of methane formation in
967   tropical anoxic lake sediments, Biogeosciences, 8, 795–814,
968   https://doi.org/10.5194/bg-8-795-2011, 2011.
969   Conrad, R., Klose, M., and Enrich-Prast, A.: Acetate turnover and methanogenic
970   pathways in Amazonian lake sediments, Biogeosciences, 17, 1063–1069,
971   https://doi.org/10.5194/bg-17-1063-2020, 2020.
972   Cranwell, P. A.: Monocarboxylic acids in lake sediments: Indicators, derived from
973   terrestrial and aquatic biota, of paleoenvironmental trophic levels, Chem Geol,
974   14, 1–14, https://doi.org/10.1016/0009-2541(74)90092-8, 1974.
975   Cranwell, P. A.: Decomposition of aquatic biota and sediment formation: organic
976   compounds in detritus resulting from microbial attack on the alga *Ceratium*
977   *hirundinella*, Freshw Biol, 6, 41–48, https://doi.org/10.1111/j.1365-
978   2427.1976.tb01589.x, 1976.
979   Dai, J., Sun, M.-Y., Culp, R. A., and Noakes, J. E.: Changes in chemical and isotopic
980   signatures of plant materials during degradation: Implication for assessing
981   various organic inputs in estuarine systems, Geophys Res Lett, 32, L13608,
982   https://doi.org/10.1029/2005GL023133, 2005.
983   Davidson, T. A., Audet, J., Jeppesen, E., Landkildehus, F., Lauridsen, T. L.,
984   Søndergaard, M., and Syväranta, J.: Synergy between nutrients and warming
985   enhances methane ebullition from experimental lakes, Nat Clim Chang, 8, 156–
986   160, https://doi.org/10.1038/s41558-017-0063-z, 2018.
987   Dean, W. E. and Gorham, E.: Magnitude and significance of carbon burial in lakes,
988   reservoirs, and peatlands, Geology, 26, 535, https://doi.org/10.3133/fs05899,
989   1998.
990   DelSontro, T., Kunz, M. J., Kempter, T., Wüest, A., Wehrli, B., and Senn, D. B.:
991   Spatial heterogeneity of methane ebullition in a large tropical reservoir, Environ
992   Sci Technol, 45, 9866–9873, https://doi.org/10.1021/es2005545, 2011.
993   Demirel, B. and Scherer, P.: The roles of acetotrophic and hydrogenotrophic
994   methanogens during anaerobic conversion of biomass to methane: a review, Rev
995   Environ Sci Biotechnol, 7, 173–190, https://doi.org/10.1007/s11157-008-9131-
996   1, 2008.
997   Downing, J. A., Prairie, Y. T., Cole, J. J., Duarte, C. M., Tranvik, L. J., Striegl, R. G.,
998   McDowell, W. H., Kortelainen, P., Caraco, N. F., Melack, J. M., and Middelburg, J. J.:
999   The global abundance and size distribution of lakes, ponds, and impoundments,
1000   Limnol Oceanogr, 51, 2388–2397, https://doi.org/10.4319/lo.2006.51.5.2388,
1001   2006.
1002   Eglinton, G. and Hamilton, R. J.: Leaf epicuticular waxes, Science (1979), 156,
1003   1322–1335, https://doi.org/10.1126/science.156.3780.1322, 1967.
1004   Ernst, L., Steinfeld, B., Barayeu, U., Klintzsch, T., Kurth, M., Grimm, D., Dick, T. P.,
1005   Rebelein, J. G., Bischofs, I. B., and Keppler, F.: Methane formation driven by
1006   reactive oxygen species across all living organisms, Nature, 603, 482–487,
1007   https://doi.org/10.1038/s41586-022-04511-9, 2022.
1008   Ficken, K. J., Li, B., Swain, D. L., and Eglinton, G.: An n-alkane proxy for the
1009   sedimentary input of submerged/floating freshwater aquatic macrophytes, Org
1010   Geochem, 31, 745–749, https://doi.org/10.1016/S0146-6380(00)00081-4,
1011   2000.

Gallina, N., Beniston, M., and Jacquet, S.: Estimating future cyanobacterial occurrence and importance in lakes: a case study with *Planktothrix rubescens* in Lake Geneva, Aquat Sci, 79, 249–263, https://doi.org/10.1007/s00027-016-0494-z, 2017.

Glombitza, C., Pedersen, J., Røy, H., and Jørgensen, B. B.: Direct analysis of volatile fatty acids in marine sediment porewater by two-dimensional ion chromatography-mass spectrometry, Limnol Oceanogr Methods, 12, 455–468, https://doi.org/10.4319/lom.2014.12.455, 2014.

Grasset, C., Mendonça, R., Villamor Saucedo, G., Bastviken, D., Roland, F., and Sobek, S.: Large but variable methane production in anoxic freshwater sediment upon addition of allochthonous and autochthonous organic matter, Limnol Oceanogr, 63, 1488–1501, https://doi.org/10.1002/lno.10786, 2018.

Han, X., Schubert, C. J., Fiskal, A., Dubois, N., and Lever, M. A.: Eutrophication as a driver of microbial community structure in lake sediments, Environ Microbiol, 22, 3446–3462, https://doi.org/10.1111/1462-2920.15115, 2020.

Han, X., Tolu, J., Deng, L., Fiskal, A., Schubert, C. J., Winkel, L. H. E., and Lever, M. A.: Long-term preservation of biomolecules in lake sediments: potential importance of physical shielding by recalcitrant cell walls, PNAS Nexus, 1, https://doi.org/10.1093/pnasnexus/pgac076, 2022.

Hansen, L. K., Jakobsen, R., and Postma, D.: Methanogenesis in a shallow sandy aquifer, Rømø, Denmark, Geochim Cosmochim Acta, 65, 2925–2935, https://doi.org/10.1016/S0016-7037(01)00653-6, 2001.

Hedges, J. I., Clark, W. A., Quay, P. D., Richey, J. E., Devol, A. H., and Santos, M.: Compositions and fluxes of particulate organic material in the Amazon River, Limnol Oceanogr, 31, 717–738, https://doi.org/10.4319/lo.1986.31.4.0717, 1986.

Jetten, M. S. M., Stams, A. J. M., and Zehnder, A. J. B.: Methanogenesis from acetate: a comparison of the acetate metabolism in *Methanothrix soehngenii* and *Methanosarcina* spp., FEMS Microbiol Lett, 88, 181–198, https://doi.org/10.1111/j.1574-6968.1992.tb04987.x, 1992.

Kawamura, K., Ishiwatari, R., and Ogura, K.: Early diagenesis of organic matter in the water column and sediments: Microbial degradation and resynthesis of lipids in Lake Haruna, Org Geochem, 11, 251–264, https://doi.org/10.1016/0146-6380(87)90036-2, 1987.

Kristensen, E., Ahmed, S. I., and Devol, A. H.: Aerobic and anaerobic decomposition of organic matter in marine sediment: Which is fastest?, Limnol Oceanogr, 40, 1430–1437, https://doi.org/10.4319/lo.1995.40.8.1430, 1995.

Kuivila, K. M., Murray, J. W., Devol, A. H., and Novelli, P. C.: Methane production, sulfate reduction and competition for substrates in the sediments of Lake Washington, Geochim Cosmochim Acta, 53, 409–416, https://doi.org/10.1016/0016-7037(89)90392-X, 1989.

Ladd, S. N., Nelson, D. B., Schubert, C. J., and Dubois, N.: Lipid compound classes display diverging hydrogen isotope responses in lakes along a nutrient gradient, Geochim Cosmochim Acta, 237, 103–119, https://doi.org/10.1016/j.gca.2018.06.005, 2018.

Lamb, A. L., Wilson, G. P., and Leng, M. J.: A review of coastal palaeoclimate and relative sea-level reconstructions using $\delta 13C$ and C/N ratios in organic material, Earth Sci Rev, 75, 29–57, https://doi.org/10.1016/j.earscirev.2005.10.003, 2006.

33

1060 Larsen, S., Andersen, T., and Hessen, D. O.: Climate change predicted to cause
1061 severe increase of organic carbon in lakes, Glob Chang Biol, 17, 1186–1192,
1062 https://doi.org/10.1111/j.1365-2486.2010.02257.x, 2011.
1063 Lehmann, M. F., Bernasconi, S. M., Barbieri, A., and McKenzie, J. A.: Preservation
1064 of organic matter and alteration of its carbon and nitrogen isotope composition
1065 during simulated and in situ early sedimentary diagenesis, Geochim Cosmochim
1066 Acta, 66, 3573–3584, https://doi.org/10.1016/S0016-7037(02)00968-7, 2002.
1067 Lehmann, M. F., Carstens, D., Deek, A., McCarthy, M., Schubert, C. J., and Zopfi, J.:
1068 Amino acid and amino sugar compositional changes during in vitro degradation
1069 of algal organic matter indicate rapid bacterial re-synthesis, Geochim Cosmochim
1070 Acta, 283, 67–84, https://doi.org/10.1016/j.gca.2020.05.025, 2020.
1071 Lever, M. A. and Teske, A. P.: Diversity of methane-cycling archaea in
1072 hydrothermal sediment investigated by general and group-specific PCR primers,
1073 Appl Environ Microbiol, 81, 1426–1441, https://doi.org/10.1128/AEM.03588-
1074 14, 2015.
1075 Li, B., Wang, H., Lai, A., Xue, J., Wu, Q., Yu, C., Xie, K., Mao, Z., Li, H., Xing, P., and
1076 Wu, Q. L.: Hydrogenotrophic pathway dominates methanogenesis along the
1077 river-estuary continuum of the Yangtze River, Water Res, 240, 120096,
1078 https://doi.org/10.1016/j.watres.2023.120096, 2023.
1079 Liu, Y. and Whitman, W. B.: Metabolic, Phylogenetic, and Ecological Diversity of
1080 the Methanogenic Archaea, Ann N Y Acad Sci, 1125, 171–189,
1081 https://doi.org/10.1196/annals.1419.019, 2008.
1082 Liu, Y., Conrad, R., Yao, T., Gleixner, G., and Claus, P.: Change of methane
1083 production pathway with sediment depth in a lake on the Tibetan plateau,
1084 Palaeogeogr Palaeoclimatol Palaeoecol, 474, 279–286,
1085 https://doi.org/10.1016/j.palaeo.2016.06.021, 2017.
1086 Lyu, Z., Shao, N., Akinyemi, T., and Whitman, W. B.: Methanogenesis, Current
1087 Biology, 28, R727–R732, https://doi.org/10.1016/j.cub.2018.05.021, 2018.
1088 Masson-Delmotte, V., Zhai, P., Pirani, A., Connors, S. L., Péan, C., Berger, S., Caud,
1089 N., Chen, Y., Goldfarb, L., and Gomis, M. I.: Climate change 2021: the physical
1090 science basis, Contribution of working group I to the sixth assessment report of
1091 the intergovernmental panel on climate change, 2, 2391, 2021.
1092 McMurdie, P. J. and Holmes, S.: Phyloseq: an R package for reproducible
1093 interactive analysis and graphics of microbiome census data, PLoS One, 8, 1–11,
1094 https://doi.org/10.1371/journal.pone.0061217, 2013.
1095 Meier, D., van Grinsven, S., Michel, A., Eickenbusch, P., Glombitza, C., Han, X.,
1096 Fiskal, A., Bernasconi, S., Schubert, C. J., and Lever, M. A.: Hydrogen–independent
1097 CO_2 reduction dominates methanogenesis in five temperate lakes that differ in
1098 trophic states, ISME Communications, 4,
1099 https://doi.org/10.1093/ismeco/ycae089, 2024.
1100 Mendonça, R., Müller, R. A., Clow, D., Verpoorter, C., Raymond, P., Tranvik, L. J.,
1101 and Sobek, S.: Organic carbon burial in global lakes and reservoirs, Nat Commun,
1102 8, 1–6, https://doi.org/10.1038/s41467-017-01789-6, 2017.
1103 Meyers, P. A.: Preservation of elemental and isotopic source identification of
1104 sedimentary organic matter, Chem Geol, 114, 289–302,
1105 https://doi.org/10.1016/0009-2541(94)90059-0, 1994.
1106 Meyers, P. A. and Ishiwatari, R.: Lacustrine organic geochemistry-an overview of
1107 indicators of organic matter sources and diagenesis in lake sediments, Org
1108 Geochem, 20, 867–900, https://doi.org/10.1016/0146-6380(93)90100-P, 1993.

Formatted: Subscript

Meyers, P. A. and Takeuchi, N.: Environmental changes in Saginaw Bay, Lake Huron recorded by geolipid contents of sediments deposited since 1800, Environmental Geology, 3, 257–266, https://doi.org/10.1007/BF02473517, 1981.

O'Leary, M. H.: Carbon isotope fractionation in plants, Phytochemistry, 20, 553–567, https://doi.org/10.1016/0031-9422(81)85134-5, 1981.

Opsahl, S. and Benner, R.: Early diagenesis of vascular plant tissues: Lignin and cutin decomposition and biogeochemical implications, Geochim Cosmochim Acta, 59, 4889–4904, https://doi.org/10.1016/0016-7037(95)00348-7, 1995.

Parsons, T. R., Stephens, K., and Strickland, J. D. H.: On the Chemical Composition of Eleven Species of Marine Phytoplankters, Journal of the Fisheries Research Board of Canada, 18, 1001–1016, https://doi.org/10.1139/f61-063, 1961.

R Core Team: A Language and Environment for Statistical Computing. (R Foundation for Statistical Computing) [online]. www.r-project.org/, 2024.

Randlett, M.-E., Sollberger, S., Del Sontro, T., Müller, B., Corella, J. P., Wehrli, B., and Schubert, C. J.: Mineralization pathways of organic matter deposited in a river–lake transition of the Rhone River Delta, Lake Geneva, Environ Sci Process Impacts, 17, 370–380, https://doi.org/10.1039/C4EM00470A, 2015.

Raymond, P. A. and Bauer, J. E.: Riverine export of aged terrestrial organic matter to the North Atlantic Ocean, Nature, 409, 497–500, https://doi.org/10.1038/35054034, 2001.

Ritalahti, K. M., Amos, B. K., Sung, Y., Wu, Q., Koenigsberg, S. S., and Löffler, F. E.: Quantitative PCR targeting 16S rRNA and reductive dehalogenase genes simultaneously monitors multiple *Dehalococcoides* strains, Appl Environ Microbiol, 72, 2765–2774, https://doi.org/10.1128/AEM.72.4.2765-2774.2006, 2006.

Rotaru, A.-E., Shrestha, P. M., Liu, F., Shrestha, M., Shrestha, D., Embree, M., Zengler, K., Wardman, C., Nevin, K. P., and Lovley, D. R.: A new model for electron flow during anaerobic digestion: direct interspecies electron transfer to Methanosaeta for the reduction of carbon dioxide to methane, Energy Environ. Sci., 7, 408–415, https://doi.org/10.1039/C3EE42189A, 2014.

Schaedler, F., Lockwood, C., Lueder, U., Glombitza, C., Kappler, A., and Schmidt, C.: Microbially mediated coupling of Fe and N cycles by nitrate-reducing Fe (II)-oxidizing bacteria in littoral freshwater sediments, Appl Environ Microbiol, 84, 1–14, https://doi.org/10.1128/AEM.02013-17, 2018.

Schellekens, J., Buurman, P., and Pontevedra-Pombal, X.: Selecting parameters for the environmental interpretation of peat molecular chemistry – A pyrolysis-GC/MS study, Org Geochem, 40, 678–691, https://doi.org/10.1016/j.orggeochem.2009.03.006, 2009.

Schubert, C. J. and Nielsen, B.: Effects of decarbonation treatments on δ13C values in marine sediments, Mar Chem, 72, 55–59, https://doi.org/10.1016/S0304-4203(00)00066-9, 2000.

Schulz, S. and Conrad, R.: Effect of algal deposition on acetate and methane concentrations in the profundal sediment of a deep lake (Lake Constance), FEMS Microbiol Ecol, 16, 251–259, https://doi.org/10.1016/0168-6496(94)00088-E, 1995.

Schulz, S. and Conrad, R.: Influence of temperature on pathways to methane production in the permanently cold profundal sediment of Lake Constance, FEMS

1157 Microbiol Ecol, 20, 1–14, https://doi.org/10.1016/0168-6496(96)00009-8,
1158 1996.
1159 Schwarz, J. I. K. K., Eckert, W., and Conrad, R.: Response of the methanogenic
1160 microbial community of a profundal lake sediment (Lake Kinneret, Israel) to
1161 algal deposition, Limnol Oceanogr, 53, 113–121,
1162 https://doi.org/10.4319/lo.2008.53.1.0113, 2008.
1163 Shi, W., Sun, M. Y., Molina, M., and Hodson, R. E.: Variability in the distribution of
1164 lipid biomarkers and their molecular isotopic composition in Altamaha estuarine
1165 sediments: Implications for the relative contribution of organic matter from
1166 various sources, Org Geochem, 32, 453–467, https://doi.org/10.1016/S0146-
1167 6380(00)00189-3, 2001.
1168 Smith, K. S. and Ingram-Smith, C.: Methanosaeta, the forgotten methanogen?,
1169 Trends Microbiol, 15, 150–155, https://doi.org/10.1016/j.tim.2007.02.002,
1170 2007.
1171 Sobek, S., Durisch-Kaiser, E., Zurbrügg, R., Wongfun, N., Wessels, M., Pasche, N.,
1172 and Wehrli, B.: Organic carbon burial efficiency in lake sediments controlled by
1173 oxygen exposure time and sediment source, Limnol Oceanogr, 54, 2243–2254,
1174 https://doi.org/10.4319/lo.2009.54.6.2243, 2009.
1175 Sobek, S., DelSontro, T., Wongfun, N., and Wehrli, B.: Extreme organic carbon
1176 burial fuels intense methane bubbling in a temperate reservoir, Geophys Res
1177 Lett, 39, 2–5, https://doi.org/10.1029/2011GL050144, 2012.
1178 Sollberger, S., Corella, J. P., Girardclos, S., Randlett, M. E., Schubert, C. J., Senn, D.
1179 B., Wehrli, B., and DelSontro, T.: Spatial heterogeneity of benthic methane
1180 dynamics in the subaquatic canyons of the Rhone River Delta (Lake Geneva),
1181 Aquat Sci, 76, 89–101, https://doi.org/10.1007/s00027-013-0319-2, 2014.
1182 Su, G., Niemann, H., Steinle, L., Zopfi, J., and Lehmann, M. F.: Evaluating
1183 radioisotope-based approaches to measure anaerobic methane oxidation rates in
1184 lacustrine sediments, Limnol Oceanogr Methods, 17, 429–438,
1185 https://doi.org/10.1002/lom3.10323, 2019.
1186 Su, G., Zopfi, J., Yao, H., Steinle, L., Niemann, H., and Lehmann, M. F.:
1187 Manganese/iron-supported sulfate-dependent anaerobic oxidation of methane
1188 by archaea in lake sediments, Limnol Oceanogr, 65, 863–875,
1189 https://doi.org/10.1002/lno.11354, 2020.
1190 Su, G., Lehmann, M. F., Tischer, J., Weber, Y., Lepori, F., Walser, J.-C., Niemann, H.,
1191 and Zopfi, J.: Water column dynamics control nitrite-dependent anaerobic
1192 methane oxidation by *Candidatus* "Methylomirabilis" in stratified lake basins,
1193 ISME J, 17, 693–702, https://doi.org/10.1038/s41396-023-01382-4, 2023.
1194 Tolu, J., Gerber, L., Boily, J.-F., and Bindler, R.: High-throughput characterization
1195 of sediment organic matter by pyrolysis–gas chromatography/mass
1196 spectrometry and multivariate curve resolution: A promising analytical tool in
1197 (paleo)limnology, Anal Chim Acta, 880, 93–102,
1198 https://doi.org/10.1016/j.aca.2015.03.043, 2015.
1199 Tolu, J., Rydberg, J., Meyer-Jacob, C., Gerber, L., and Bindler, R.: Spatial variability
1200 of organic matter molecular composition and elemental geochemistry in surface
1201 sediments of a small boreal Swedish lake, Biogeosciences, 14, 1773–1792,
1202 https://doi.org/10.5194/bg-14-1773-2017, 2017.
1203 Valentine, D. W., Holland, E. A., and Schimel, D. S.: Ecosystem and physiological
1204 controls over methane production in northern wetlands, J Geophys Res, 99,
1205 1563, https://doi.org/10.1029/93JD00391, 1994.

Formatted: Font: Italic

Deleted: Team, R. C.: A Language and Environment for Statistical Computing. (R Foundation for Statistical Computing) [online], www.r-project.org/, 2024.¶

Volkman, J. K.: A review of sterol markers for marine and terrigenous organic matter, Org Geochem, 9, 83–99, https://doi.org/10.1016/0146-6380(86)90089-6, 1986.

Volkman, J. K., Johns, R. B., Gillan, F. T., Perry, G. J., and Bavor, H. J.: Microbial lipids of an intertidal sediment—I. Fatty acids and hydrocarbons, Geochim Cosmochim Acta, 44, 1133–1143, https://doi.org/10.1016/0016-7037(80)90067-8, 1980.

Volkman, J. K., Barrett, S. M., Blackburn, S. I., Mansour, M. P., Sikes, E. L., and Gelin, F.: Microalgal biomarkers: A review of recent research developments, Org Geochem, 29, 1163–1179, https://doi.org/10.1016/S0146-6380(98)00062-X, 1998.

West, W. E., Coloso, J. J., and Jones, S. E.: Effects of algal and terrestrial carbon on methane production rates and methanogen community structure in a temperate lake sediment, Freshw Biol, 57, 949–955, https://doi.org/10.1111/j.1365-2427.2012.02755.x, 2012.

West, W. E., McCarthy, S. M., and Jones, S. E.: Phytoplankton lipid content influences freshwater lake methanogenesis, Freshw Biol, 2261–2269, https://doi.org/10.1111/fwb.12652, 2015.

Whiticar, M. J.: Carbon and hydrogen isotope systematics of bacterial formation and oxidation of methane, Chem Geol, 161, 291–314, https://doi.org/10.1016/S0009-2541(99)00092-3, 1999.

Whiticar, M. J. J., Faber, E., and Schoell, M.: Biogenic methane formation in marine and freshwater environments: CO_2 reduction vs. acetate fermentation—Isotope evidence, Geochim Cosmochim Acta, 50, 693–709, https://doi.org/10.1016/0016-7037(86)90346-7, 1986.

Xiao, K.-Q., Beulig, F., Røy, H., Jørgensen, B. B., and Risgaard-Petersen, N.: Methylotrophic methanogenesis fuels cryptic methane cycling in marine surface sediment, Limnol Oceanogr, 63, 1519–1527, https://doi.org/10.1002/lno.10788, 2018.

Xu, L., Zhuang, G. C., Montgomery, A., Liang, Q., Joye, S. B., and Wang, F.: Methyl-compounds driven benthic carbon cycling in the sulfate-reducing sediments of South China Sea, Environ Microbiol, 23, 641–651, https://doi.org/10.1111/1462-2920.15110, 2021.

Zhao, B., Ma, J., Zhao, Q., Laurens, L., Jarvis, E., Chen, S., and Frear, C.: Efficient anaerobic digestion of whole microalgae and lipid-extracted microalgae residues for methane energy production, Bioresour Technol, 161, 423–430, https://doi.org/10.1016/j.biortech.2014.03.079, 2014.

Zhou, J., Smith, J. A., Li, M., and Holmes, D. E.: Methane production by *Methanothrix thermoacetophila* via direct interspecies electron transfer with *Geobacter metallireducens*, mBio, 2–3, https://doi.org/10.1128/mbio.00360-23, 2023.

Zhuang, G.-C., Heuer, V. B., Lazar, C. S., Goldhammer, T., Wendt, J., Samarkin, V. A., Elvert, M., Teske, A. P., Joye, S. B., and Hinrichs, K.-U.: Relative importance of methylotrophic methanogenesis in sediments of the Western Mediterranean Sea, Geochim Cosmochim Acta, 224, 171–186, https://doi.org/10.1016/j.gca.2017.12.024, 2018.